International Journal of Researches on Civil Engineering with Artificial Intelligence

www.ceai.reapress.com

Int. J. Res. Civ. Eng. AI. Vol. 3, No. 1 (2026) 51–77.

Paper Type: Original Article

Thermo-Mechanical Buckling Analysis of Polymer Nanocomposite Beams Reinforced with Carbon Nanotubes Considering Interphase Effects via Finite Element Modeling

Mehdi Moslemi[1,*], Khadijeh Ghaziyani[2], Fatemeh Nejati[3]

[1] Department of Mechanical Engineering, Ayandegan University, Tonekabon, Iran; mehdimoslemi1982@gmail.com.
[2] Department of Mathematics, Ayandegan University, Tonekabon, Iran; ghaziyani89@gmail.com.
[3] Department of Civil, Architecture and Arts, Science and Research Branch, Islamic Azad University, Tehran, Iran; archi_fania@yahoo.com.

Citation:

Received: 25 March 2025 *Revised: 10 May 2025* *Accepted: 16 July 2025*	Moslemi, M., Ghaziyani, Kh., & Nejati, F. (2026). Thermo-mechanical buckling analysis of polymer nanocomposite beams reinforced with carbon nanotubes considering interphase effects via finite element modeling. *International Journal of Researches on Civil Engineering with Artificial Intelligence, 3*(1), 51-77.

Abstract

This study investigates the buckling behavior of polymer-matrix nanocomposite beams reinforced with Carbon Nanotubes (CNTs) using the Finite Element Method (FEM) in combination with an analytical micromechanical model. The effective mechanical properties elastic modulus, shear modulus, and Poisson's ratio are first determined through the Mori Tanaka approach. Both aligned and random CNT dispersion states are considered. A distinct feature of this modeling is the inclusion of the interphase region arising from non-bonded van der Waals interactions between CNTs and the polymer matrix. The interphase is characterized by its thickness and an adhesion exponent, which together control the quality of interfacial bonding. After obtaining the homogenized elastic properties, they are imported into ABAQUS to perform buckling analysis of a cantilever nanocomposite beam (length 1 m, square cross-section 0.1×0.1 m) subjected to a unit pressure load. The beam is discretized using 20-node quadratic brick elements (C3D20) after verifying mesh convergence. A comprehensive parametric study examines the influence of CNT volume fraction (0–5%), CNT diameter (0.5–4 nm), temperature (260–350 K), interphase thickness (0.1–1.3 nm), adhesion exponent (0.01–95), and beam dimensions on the critical buckling load. Results show that increasing CNT volume fraction dramatically enhances the buckling load. For example, the first-mode buckling load increases from 2.65 MPa for the pure polymer to 45.1 MPa at 5 vol.% CNTs when the interphase is included a 17-fold improvement, significantly delaying buckling failure. Elevated temperature reduces the buckling load due to matrix softening. The interphase plays a crucial role: when included, decreasing CNT diameter (which increases the interphase volume fraction) substantially raises the buckling load; without the interphase, diameter has no effect. Increasing interphase thickness or decreasing the adhesion exponent (making the interphase stiffer) also improves buckling resistance. Longer beams and larger cross-sections show expected trends of lower and higher buckling loads, respectively. For higher vibration modes (e.g., mode 5), hollow cross-sections can exhibit higher buckling loads than solid ones. Validation against experimental data from the literature confirms that the proposed micromechanical model offers acceptable accuracy. These findings provide practical guidelines for designing CNT-reinforced nanocomposite beams with enhanced buckling resistance.

Keywords: Nanocomposite beam, Carbon nanotube, Buckling, Micromechanics.

1 | Introduction

The continuous advancement of industries across fields such as aerospace, marine engineering, power generation, automotive manufacturing, petrochemicals, medicine, and others has led to a significant increase

Corresponding Author: mehdimoslemi1982@gmail.com
https://doi.org/10.48314/ijrceai.v3i1.42

in demand for structural materials with improved performance in engineering applications under various loading and environmental conditions. Therefore, designers have always been compelled to develop new materials with unique characteristics and superior capabilities.

Over the last two decades, nanoscience and nanoengineering have experienced remarkable growth, and research in this field spans a wide range of material systems and applications. Composite materials reinforced with nanoscale phases are among the practical products of nanotechnology that have gained considerable importance and are among the active research areas. Worldwide interest in nanoparticle-reinforced composite materials has motivated many research centers, scientific institutions, and companies to investigate their potential capabilities and practical applications. In the development of advanced composite materials, the reinforcing agent has shifted from the microscale toward the nanoscale. These composite materials exist in various forms, including nanoparticle-reinforced nanocomposites (e.g., silica nanoparticles), nanoplatelet-reinforced composites (e.g., graphite), and Carbon Nanotube (CNT)-reinforced composites [1]. Nanocomposites have attracted the attention of many researchers because they provide a platform for designing materials with superior, often novel and multifunctional, properties. Among nanoparticles, CNTs have received more attention than other nanoparticles due to their excellent mechanical, thermal, and electrical properties, as well as their low density and high aspect ratio (length-to-diameter ratio). Previous studies have shown that adding only 1 wt.% of CNTs to a polystyrene matrix increases the elastic modulus of the resulting nanocomposite by 36–42%. At the same time, its mechanical strength improves by up to 25% [2].

Shokrieh et al. [3] fabricated epoxy-matrix nanocomposite specimens containing CNTs with weight fractions of 0.1%, 0.5%, and 1%. Experimental reports indicated that the thermoelastic coefficient of the epoxy-matrix nanocomposite reinforced with 0.1%, 0.5%, and 1 wt.% CNTs decreased by 6%, 21%, and 23.7%, respectively, compared with the pure polymer. Kalmolah et al. [4] also investigated the thermoelastic coefficient of polybenzoxazine-matrix nanocomposites reinforced with CNTs. Stern and Marom [5] experimentally examined the effect of multiwalled CNTs on the fracture resistance of epoxy-matrix nanocomposites under out-of-plane shear loading (Mode III fracture) in comparison with tensile loading (Mode I fracture). The results showed that, in both loading conditions, increasing the nanotube content to 1 wt.% enhanced the fracture resistance relative to pure epoxy. However, the maximum Mode I and Mode III fracture toughness values were obtained for nanocomposites containing 0.5 wt.% and 1 wt.% nanotubes, respectively.

Theoretical studies conducted on CNT-reinforced composite materials can generally be classified into three major categories: atomic modeling [6], multiscale modeling [7], and micromechanical modeling [8], [9]. Sahu et al. [10] investigated the mechanical properties of unidirectional CNT-reinforced polymer-matrix nanocomposites using a micromechanical finite element approach and a square Representative Volume Element (RVE). The results showed that adding 3.6 vol.% CNTs to the polymer matrix increased the Young's modulus of the nanocomposite by 33%. In addition, Wan et al. [11] used a micromechanical finite element model to study the effects of CNT length and the interphase between the nanotube and the resin on the mechanical properties of the nanocomposite. They reported that the reinforcing effect of long nanotubes in the nanocomposite was greater than that of short nanotubes. Karimi et al. [12] investigated the elastoplastic properties of a polymer-matrix nanocomposite based on several microscale parameters. Their examination of nanotube length revealed that nanotubes with lengths ranging from 10 to 300 nm had a significant effect on the Young's modulus of the nanocomposite.

In contrast, neither shorter nor longer lengths had a substantial influence. Esbati and Irani [13] evaluated the factors affecting the mechanical properties and failure mechanisms of polymer nanocomposites reinforced with pristine and functionalized CNTs. They found that, depending on factors such as the distribution, distortion, and functionalization of CNTs, the strength of polymer nanocomposites may either decrease or increase relative to the pure polymer.

Using the finite element micromechanical method, Hammerrand et al. [14] estimated the elastic modulus, shear modulus, and Poisson's ratio in the longitudinal and transverse directions for epoxy-matrix nanocomposites reinforced with straight CNTs. Their reports indicated that the elastic properties obtained from the two modeling approaches were very similar. Zhang and He [15], employing the analytical micromechanical concentric-cylinder model, estimated the longitudinal Young's modulus of CNT-reinforced epoxy-matrix nanocomposites. The results clearly demonstrated that the nanocomposite's mechanical properties were not affected by the nanotube aspect ratio. Mehrdad Shokrieh et al. [16] considered a RVE consisting of a surrounding polymer matrix and a CNT core, both rectangular prisms with square cross-sections. Mahmoudi and Vakilifard [17] developed and extended a three-dimensional analytical micromechanical model based on a unit cell for extracting the mechanical, thermal, and electrical properties of piezopolymer nanocomposites reinforced with CNTs. Tsai et al. [18] also considered CNTs as transversely isotropic materials. Using molecular dynamics simulations, they obtained five elastic constants for CNTs with different radii. Tserpes and Papanikos [19] presented three-dimensional finite element models for armchair, zigzag, and chiral single-walled CNTs to investigate the effects of diameter and wall thickness on the elastic modulus of CNTs. Ressi and Meo [20] used molecular mechanics to propose a finite element model for evaluating the mechanical properties of CNTs. Ansari et al. [21] studied the mechanical properties and buckling behavior of CNTs through molecular dynamics simulations. The elastic properties of CNT-reinforced composites were predicted through micromechanical analysis by Tserpes and Chou [22]. Han and Elliott [23] investigated the effects of the volume fraction of single-walled nanotubes on the mechanical properties of polymer-matrix nanocomposites. They showed that when the interaction between CNTs and the polymer matrix is strong, the interphase effects must be considered in modeling these materials.

Sahu et al. [10] proposed a finite element model based on a square RVE to extract the mechanical properties of CNT-reinforced composites. Griebel and Hamaekers [24] used molecular dynamics simulations to predict the elastic modulus of polyethylene-matrix nanocomposites reinforced with single-walled CNTs. The results of their study showed that for continuous CNTs, the longitudinal elastic modulus of the nanocomposite agreed well with that predicted by the micromechanical rule-of-mixtures model. Joshi and Upadhyay [9], using the Finite Element Method (FEM) and considering a RVE composed of three phases, including a straight CNT, matrix, and interphase, evaluated the elastic modulus of unidirectional nanocomposites. In this numerical micromechanical model, the interphase was assumed to be a coating layer of specified thickness located on the nanotube's outer surface. Variations in the elastic modulus of the interphase within the range of 0.5 to 5.5 times the elastic modulus of the matrix were considered to represent soft and stiff interphases, respectively. The effects of nanotube volume fraction and length, interphase thickness, and the elastic properties of the interphase and matrix on the Young's modulus of aligned nanotube-reinforced nanocomposites were analyzed.

Wang and Liu [25] proposed a numerical micromechanical model based on the meshfree method to predict the elastic behavior of nanocomposites containing straight CNTs. In this approach, a three-dimensional cylindrical RVE was considered, in which both the CNT and matrix were modeled as isotropic materials. The influence of the matrix elastic modulus on the mechanical properties, including elastic moduli and Poisson's ratios in the longitudinal and transverse directions for unidirectional nanocomposites, was numerically investigated. The results indicated that the longitudinal elastic modulus increased linearly with increasing CNT volume fraction, whereas the transverse elastic modulus increased nonlinearly.

Pan et al. [26] combined the Mori–Tanaka micromechanical model with the rule of mixtures to investigate the effects of agglomeration and waviness of CNTs on the effective elastic properties of polymer-matrix nanocomposites. Their results showed that the mechanical properties of the nanocomposite are sensitive to nanotube waviness and agglomeration when dispersion within the polymer matrix is non-uniform. Imani Yengejeh et al. [27] conducted a comprehensive review of theoretical and experimental methods for determining the effective properties of CNT-containing nanocomposites. A major part of their review focused on the micromechanical modeling of nanocomposites using RVEs. Karimi et al. [28] used the FEM

to investigate the effect of nanotube/resin interfacial debonding on the mechanical behavior of nanocomposites.

Research has also been conducted on the mechanical behavior of structures made of CNT-reinforced nanocomposites, including bending, buckling, and vibration analyses. Vodenitcharova and Zhang [29] investigated the bending and buckling behavior of nanocomposite beams reinforced with single-walled CNTs using the Airy stress function. The buckling of CNT-reinforced nanocomposite plates under uniaxial compressive loading and thermal loading was developed by Shen et al. [30]. He obtained the properties of the nanocomposite plate using the modified rule of mixtures. He also showed that the use of linearly graded CNTs as the reinforcing phase in nanocomposites increases the critical bending load. Torabi et al. [31] studied the thermal buckling of composite conical shells reinforced with functionally distributed CNTs. The results showed that the nanotube volume fraction and the distribution of CNT type through the thickness direction have a significant effect on the thermal stability of conical shells made of nanocomposite materials.

Zhu et al. [32] extended the FEM to investigate the bending and free vibration behavior of CNT-reinforced nanocomposite plates. They used the modified rule of mixtures to estimate the composite plate's properties. In another study, Lei et al. [33] developed a mesh-free method for buckling analysis of CNT-reinforced nanocomposite plates based on the first-order shear deformation theory. They also employed the modified rule of mixtures in their study. Jafari Mehrabadi et al. [34] used the first-order shear deformation theory to present a biaxial buckling analysis of CNT-reinforced nanocomposite plates. They concluded that the critical biaxial buckling load increases with both the thickness-to-width ratio and the CNT volume fraction. Shaat et al. [35] presented a size-dependent analysis of bending, buckling, and vibration of nanoplates based on the modified couple-stress theory, incorporating surface stress effects. They also derived an analytical solution for static bending using couple stress theory.

Malekzadeh and Shojaei [36] studied the buckling analysis of multilayer plates reinforced with CNTs. They investigated the effects of CNT volume fraction, thickness-to-length ratio, different nanotube distributions, and various boundary conditions on the critical buckling load of multilayer plates. Mahmoudi Mehr et al. [37] used the couple stress theory to investigate size-dependent effects on the buckling and vibration analysis of piezoelectric nanocomposite plates. Ansari et al. [38] studied the vibration and buckling behavior of functionally graded CNT-reinforced composite plates under thermal loading. The mechanical and thermal properties of this nanocomposite were determined using the rule-of-mixtures approach. Furthermore, Farzam and Hassani [39] presented a mechanical and thermal buckling analysis of functionally graded CNT-reinforced nanocomposites using the isogeometric method based on the modified couple-stress theory. In their analysis, the nanocomposite's material properties were considered temperature-dependent.

The objective of the present study is to investigate the buckling behavior of beams made of CNT-reinforced nanocomposites. For this purpose, the equivalent mechanical properties of the CNT-reinforced nanocomposite are first obtained using the analytical micromechanical Mori–Tanaka model equations. These properties include the elastic modulus, Poisson's ratio, and shear modulus. Subsequently, these mechanical properties are introduced as input data into the finite element software ABAQUS in order to analyze the buckling behavior of the nanocomposite beam. The effects of nanotube volume fraction, geometry, and dispersion state on the effective properties of CNT-reinforced nanocomposites are analyzed. Finally, the buckling behavior of nanotube-reinforced nanocomposite beams is investigated and discussed.

2 | Modeling of Carbon Nanotube-Reinforced Nanocomposite Beams

For any mechanical behavior analysis of structures, it is first necessary to determine the material's effective properties. Therefore, in this section, the Mori–Tanaka micromechanical model for extracting the mechanical properties of CNT-reinforced nanocomposites is first presented. Then, the modeling procedure for the buckling behavior of a nanocomposite beam made of this nanocomposite material is described.

2.1 | Mori–Tanaka Micromechanical Model

In this section, the Mori–Tanaka micromechanical model is presented for determining the mechanical properties of equivalent nanofiber, aligned CNT-reinforced, and randomly oriented CNT-reinforced nanocomposites.

In previous studies, an equivalent solid continuum material, referred to as the interphase, has been used to model van der Waals interactions between nanotube atoms and the polymer matrix in micromechanical modeling. *Fig. 1* illustrates a schematic representation of the RVE of a polymer-matrix nanocomposite reinforced with a straight CNT, together with the interphase. As shown in *Fig. 1.(a)*, the CNT is surrounded by an interphase with constant thickness. *Fig. 1.(b)* presents the longitudinal cross-section of this RVE.

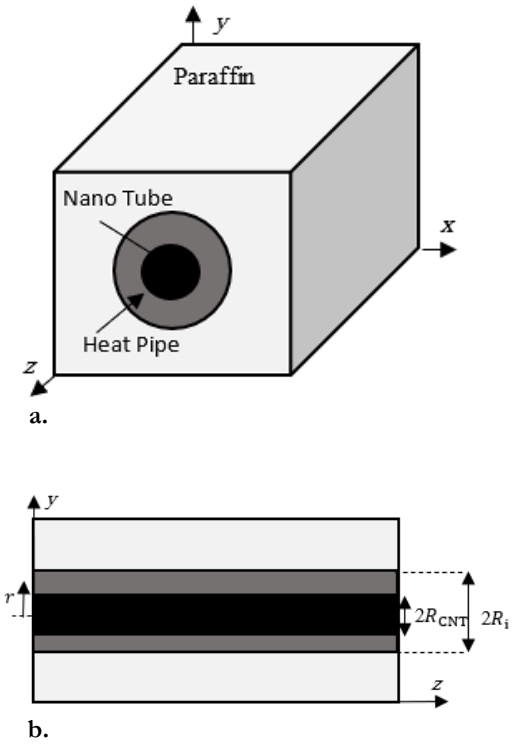

Fig. 1. a. schematic representation of the RVE of a polymer-matrix nanocomposite reinforced with a straight and long CNT together with the interphase, and b. longitudinal cross-section of the RVE.

In order to calculate the elastic properties of the interphase, the following function is used to determine the elastic stiffness matrix of the interphase:

$$\mathbf{C}^{i} = \frac{1}{t_i}\int_{\frac{d}{2}}^{\frac{d}{2}+t_i} \mathbf{C}^{p}\left(\frac{\frac{d}{2}+t_i}{r}\right) + \left(\frac{\frac{d}{2}+t_i-r}{t_i}\right)^{\eta}\left[\mathbf{C}^{CNT} - \mathbf{C}^{p}\left(\frac{\frac{d}{2}+t_i}{\frac{d}{2}}\right)\right] dr. \quad (1)$$

In *Eq. (1)*, C^{CNT}, C^{p}, and Cidenote the elastic stiffness matrices of the CNT, polymer matrix, and interphase, respectively. Moreover, d represents the nanotube diameter. In the above relations, t_i and η are, respectively, the interphase thickness and the adhesion exponent, which control the quality of bonding in the interfacial layer between the CNT and the polymer matrix.

Therefore, the CNT and the interphase are first combined to form an equivalent nanofiber. The elastic properties of this equivalent nanofiber are obtained using the Mori–Tanaka method, considering the nanotube as the reinforcement phase and the interphase as the matrix phase, according to the following relation:

$$C^{r} = C^{i} + f_n\langle\left(C^{CNT} - C^{i}\right)A_r\rangle\left(f_i I + f_n\langle A_r\rangle\right)^{-1}, \quad (2)$$

where f_n and f_i are the volume fractions of the nanotube and the interphase, respectively. In addition, I is the fourth-order identity tensor. In the above equation, A^r is is defined as

$$A_r = [I + S(C^i)^{-1}(C^{CNT} - C^i)^{-1}, \quad (3)$$

where S is the Eshelby tensor, the nonzero coefficients of the Eshelby tensor are given as follows.

$$S_{2222} = S_{3333} = \frac{5 - 4v_i}{8(1 - v_i)},$$
$$S_{2211} = S_{3311} = \frac{v_i}{2(1 - v_i)},$$
$$S_{1212} = S_{1313} = \frac{1}{4}, \quad (4)$$
$$S_{2233} = S_{3322} = \frac{4v_i - 1}{8(1 - v_i)},$$
$$S_{3311} = \frac{3 - 4v_i}{8(1 - v_i)},$$

where v_i is the Poisson's ratio of the interphase. It should be noted that the CNT is considered a solid cylindrical fiber. Therefore, as the first step, the elastic properties, including the stiffness tensor, of the equivalent nanofiber composed of a CNT and the interphase are calculated.

2.2|Nanocomposite Reinforced with Aligned Carbon Nanotubes

Using the elastic properties of the nanofiber obtained in the previous section together with those of the polymer matrix, the Mori–Tanaka method can be employed to estimate the effective elastic coefficient matrix of the nanocomposite reinforced with aligned CNTs. *Fig. 2* presents a schematic illustration of a nanocomposite reinforced with aligned CNTs.

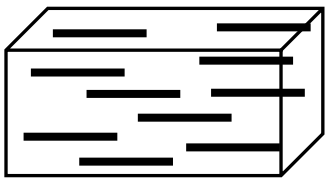

Fig. 2. Schematic representation of a nanocomposite reinforced with aligned CNTs.

Based on the Mori–Tanaka method, the stress–strain relationship in the elastic region for the nanocomposite is expressed as follows:

$$\sigma^{nc} = C^{nc}\varepsilon^{nc}, \quad (5)$$

where the elastic stiffness tensor of the nanocomposite can be written as:

$$C^{nc} = C^m + f_r(C^r - C^m)A_1. \quad (6)$$

In *Eq. (6)*, f_r is the volume fraction of the nanofiber and C^m is is the elastic stiffness tensor of the polymer matrix. The strain concentration factor matrix is obtained as follows:

$$A_1 = \hat{A}_1 + \left[(1 - f_r)I + f_r\hat{A}_1\right]^{-1}. \quad (7)$$

$$\hat{A}_1 = \left[I + \hat{S}[C^m]^{-1}([C^r] - [C^m])\right]^{-1}. \quad (8)$$

The special form of the Eshelby tensor for the cylindrical case, which is used for calculating the components of the tensor S, is given by:

$$s_{2222} = s_{3333} = \frac{5 - 4v_m}{8(1 - v_m)}.$$
$$s_{2233} = s_{3322} = \frac{4v_m - 1}{8(1 - v_m)}.$$
$$s_{2211} = s_{3311} = \frac{v_m}{2(1 - v_m)}. \quad (9)$$
$$s_{1212} = s_{1313} = \frac{1}{4}.$$
$$s_{2323} = \frac{3 - 4v_m}{8(1 - v_m)}.$$

Fig. 3 shows a schematic representation of a nanocomposite reinforced with randomly dispersed CNTs. Based on the Mori–Tanaka method, the elastic coefficient tensor of a nanocomposite containing randomly oriented nanotubes, C^{RO}, is given by:

$$C^{RO} = C^{P} + f_r \langle T \rangle.$$
$$T = (C^r - C^m).[I + S.((C^m)^{-1}.C^m - I)]^{-1}. \quad (10)$$

In this relation, T denotes the orientational averaging of a fourth-order tensor, which is defined as:

$$\langle T \rangle_{ijkl} = \frac{1}{\pi}\int_0^{\pi}\left(\int_0^{\pi/2} Q_{ip}Q_{jq}Q_{kr}Q_{ls}T_{pqrs}\cos\varphi\, d\varphi\right) d\gamma, \quad (11)$$

where the transformation tensor Q is expressed as:

$$Q = \begin{bmatrix} \cos\gamma\ \cos\varphi & \sin\varphi & \cos\gamma\ \sin\varphi \\ -\cos\varphi\ \sin\gamma & \cos\gamma & -\sin\varphi\ \sin\gamma \\ -\sin\varphi & 0 & \cos\varphi \end{bmatrix}. \quad (12)$$

In fact, the transformation tensor defines the relationship between the coordinate systems $o - x_1x_2x_3$ and o-x1x2x$o - x_1x_2x_3$ as illustrated in *Fig. 3*.

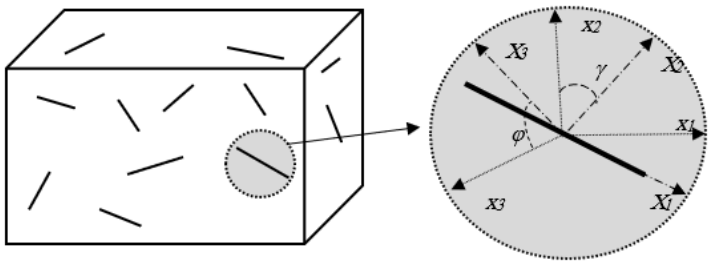

Fig. 3. RVE of a nanocomposite containing straight CNTs with random orientation.

After substituting the equation into *Eq. (11)* and then substituting the result into *Eq. (10)*, the shear modulus and bulk modulus of the polymer-matrix nanocomposite reinforced with randomly dispersed CNTs can be expressed as follows:

$$K^{nc} = K_m + \frac{f_r(\delta_r - 3K_m\alpha_r)}{3(f_m + f_r\alpha_r)}, \quad (13)$$

$$G^{nc} = G_m + \frac{f_r(\eta_r - 2G_m\beta_r)}{2(f_m + f_r\beta_r)}, \tag{14}$$

where K_m and G_m are are respectively the bulk modulus and shear modulus of the polymer matrix. In addition, fm is the volume fraction of the polymer matrix. The coefficients δ_r, α_r, η_r, and β_r are expressed as follows:

$$\alpha_r = \frac{3(K_m + G_m) + k_r - l_r}{3(G_m + k_r)}. \tag{15}$$

$$\beta_r = \frac{1}{5}\left\{\frac{4G_m + 2k_r + l_r}{3(G_m + k_r)} + \frac{4G_m}{G_m + p_r} + \frac{2[G_m(3K_m + G_m) + G_m(3K_m + 7G_m)]}{G_m(3K_m + G_m) + m_r(3K_m + 7G_m)}\right\}. \tag{16}$$

$$\delta_r = \frac{1}{3}\left[n_r + 2l_r + \frac{(2k_r + l_r)(3K_m + 2G_m - l_r)}{G_m + k_r}\right]. \tag{17}$$

$$\eta_r = \frac{1}{5}\left[\frac{2}{3}(n_r - l_r) + \frac{8G_m p_r}{G_m + p_r} + \frac{8m_r G_m(3K_m + 4G_m)}{3K_m(m_r + G_m) + G_m(7m_r + G_m)} + \frac{2(k_r - l_r)(2G_m + l_r)}{3(G_m + k_r)}\right]. \tag{18}$$

In the above relations, k_r, l_r, n_r, m_r and p_r are Hill's coefficients, which are obtained from the following relation:

$$C^r = \begin{bmatrix} n_r & l_r & l_r & 0 & 0 & 0 \\ l_r & k_r + m_r & k_r - m_r & 0 & 0 & 0 \\ l_r & k_r - m_r & k_r + m_r & 0 & 0 & 0 \\ 0 & 0 & 0 & p_r & 0 & 0 \\ 0 & 0 & 0 & 0 & m_r & 0 \\ 0 & 0 & 0 & 0 & 0 & p_r \end{bmatrix}. \tag{19}$$

It should be noted that the components of the tensor C^r are are obtained from *Eq. (2)*. In fact, the tensor C^r represents the stiffness coefficients of the equivalent nanofiber, which is considered as a transversely isotropic material.

Finally, the elastic modulus and Poisson's ratio of the polymer-matrix nanocomposite containing CNTs can be expressed as follows:

$$E^{nc} = \frac{9K^{cn}G^{nc}}{3K^{nc} + G^{nc}}, \qquad \nu^{nc} = \frac{3K^{nc} - 2G^{nc}}{6K^{nc} + 2G^{nc}}. \tag{20}$$

3 | Numerical Solution Method for Buckling Analysis

After analyzing the equivalent mechanical properties of the CNT-reinforced nanocomposite and applying them to the desired structure, its buckling behavior is investigated using the FEM.

In this study, the beam is made of a nanocomposite material containing CNTs. The beam length is 1 meter, and its cross-sectional area is 1.0 × 1.0. *Fig. 4* presents a schematic representation of the beam in two different views.

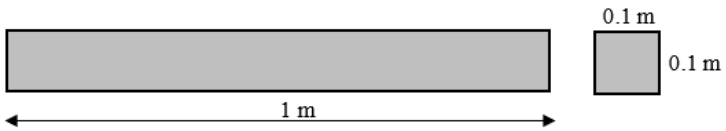

Fig. 4. Schematic representation of the beam in two views.

In this study, ABAQUS finite element software version 6.12 is employed. It should be noted that the modeling carried out in ABAQUS is three-dimensional. The boundary conditions considered for the beam are such that displacement and rotation are constrained at one end. In other words, a clamped boundary condition is assumed. Furthermore, the loading condition is defined by applying a unit pressure on the initial surface of the beam. *Fig. 5* illustrates the boundary and loading conditions, as well as the three-dimensional model of the beam.

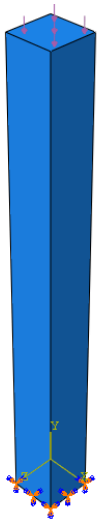

Fig. 5. Boundary conditions and loading of the beam.

For meshing the nanocomposite beam, the element type C3D20: a 20-node quadratic brick is used. The element size is considered to be 0.01 . This size is selected such that the results do not exhibit noticeable dependence on the mesh dimensions; in other words, a convergence trend is observed. It should be noted that the mechanical properties are extracted using the Mori–Tanaka method presented in Section 2 of this paper and are then assigned to the beam. Finally, after meshing the structure, the buckling behavior analysis is performed.

4 | Results

4.1 | Validation of the Micromechanical Model

In this section, the results of the mechanical properties of the CNT-reinforced polymer-matrix nanocomposite are first presented. Subsequently, the buckling behavior of a beam made from this nanocomposite material is investigated, considering various geometric and material parameters.

First, a comparison is made between the Mori–Tanaka (M–T) micromechanical method and the Eshelby method. The comparison concerns an epoxy-matrix nanocomposite reinforced with CNTs. These nanotubes are randomly dispersed within the polymer matrix. The elastic modulus of the CNTs and the polymer matrix are 1000 GPa and 3 GPa, respectively. In addition, the Poisson's ratio of both materials is equal to 0.3. *Fig. 6* illustrates this comparison.

In this figure, the normalized elastic modulus of the nanocomposite relative to the matrix elastic modulus is plotted as a function of the CNT volume fraction. EEE denotes the modulus of the nanocomposite, while ey represents the matrix modulus. At first glance, there is clear agreement between the two methods, indicating the Mori–Tanaka model is accurate. From *Fig. 6*, it can be concluded that increasing the volume fraction of CNTs leads to an increase in the elastic stiffness of the nanocomposite. In other words, increasing the amount of CNTs can improve their properties. The reason for this behavior is that the mechanical properties (including the elastic modulus) of CNTs are significantly higher than those of the polymer matrix.

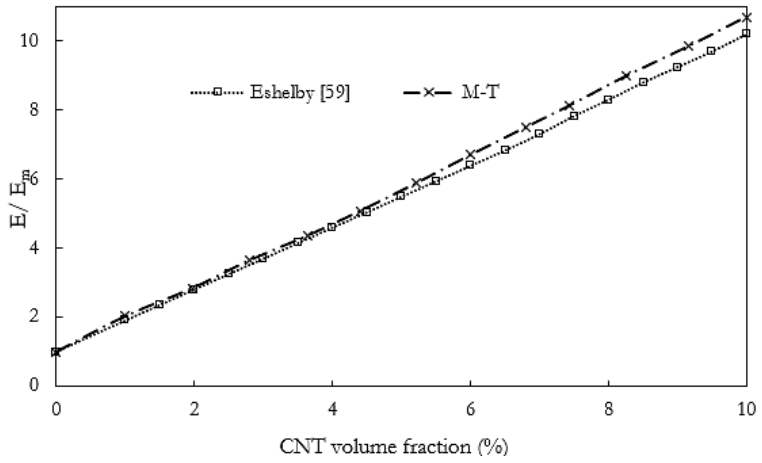

Fig. 6. Comparison between the Mori–Tanaka method and the Eshelby method for the elastic modulus of the nanocomposite.

Next, the Mori–Tanaka micromechanical model is validated using experimental data for the mechanical properties of an epoxy-matrix nanocomposite reinforced with CNTs. The properties of the CNTs and the epoxy matrix are given in *Table 1*. In this table, E_L and E_T denote the longitudinal and transverse elastic moduli, respectively. Similarly, v_L and v_T represent the longitudinal and transverse Poisson's ratios, respectively. The average diameter of the CNTs is 39 nm. In addition, the interphase thickness and adhesion exponent are considered to be 8 nm and 3.15, respectively.

Fig. 7 shows a comparison between the longitudinal elastic modulus of an epoxy-matrix nanocomposite reinforced with unidirectional CNTs obtained from the Mori–Tanaka method and the experimental results reported by Shirasu et al. [40]. In general, the results indicate that the elastic modulus predicted by the present micromechanical model is in good agreement with the experimental data. It is also observed that the nanocomposite's longitudinal elastic modulus increases linearly with increasing CNT volume fraction.

Table 1. Mechanical properties of CNTs and epoxy resin.

Material	E_L (GPa)	E_T (GPa)	v_L	v_T
CNT	240	50	0.162	0.47
Epoxy	2.5	2.5	0.34	0.34

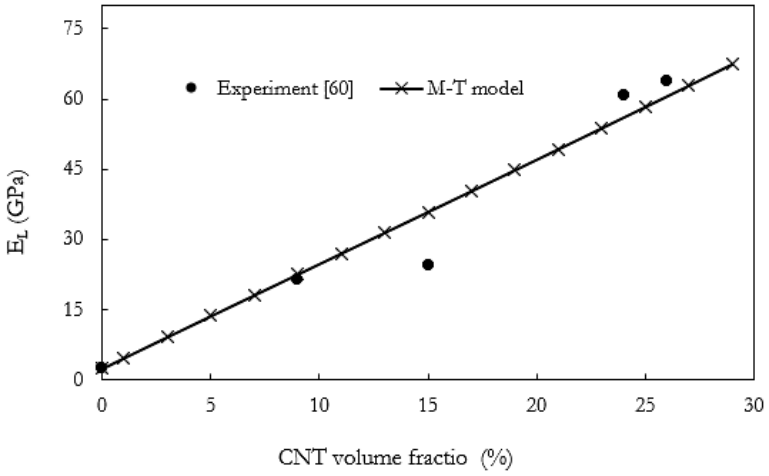

Fig. 7. Comparison between the Mori–Tanaka method and experimental results for the elastic modulus of an epoxy-matrix nanocomposite reinforced with aligned CNTs.

Another comparison is made between the Mori–Tanaka micromechanical method used in this study and the Simplified Unit Cell (SUC) micromechanical approach. This comparison presents the longitudinal elastic modulus of a shape-memory polymer matrix nanocomposite reinforced with aligned CNTs. The elastic modulus and Poisson's ratio of the polymer matrix are 0.622 GPa and 0.3, respectively.

Fig. 8 compares these two micromechanical models. It is clearly observed that there is acceptable agreement between the two approaches. The results also indicate that increasing the amount of CNTs increases the nanocomposite's elastic modulus.

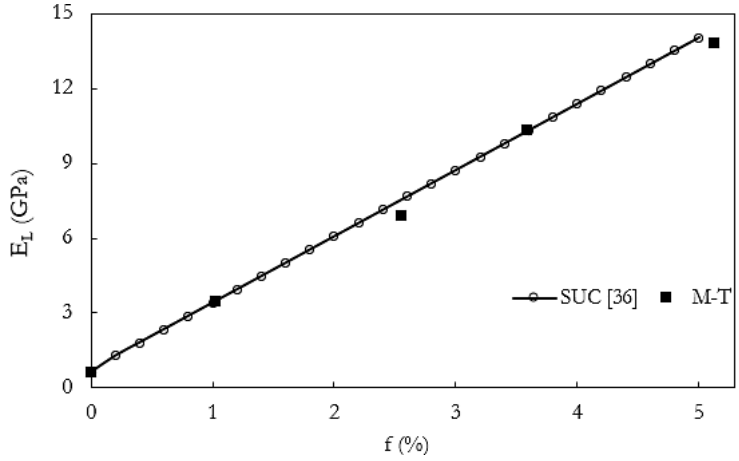

Fig. 8. Comparison between the Mori–Tanaka method and the unit cell method for the elastic modulus of the nanocomposite.

Another comparison is made between the Mori–Tanaka micromechanical method results and the experimental data reported in [23] for the mechanical properties of a polypropylene-matrix nanocomposite containing CNTs. The dispersion of nanotubes within the polymer matrix is assumed to be random. Therefore, the micromechanical relations developed in Section 2 are employed.

The mechanical properties of the CNTs are given in *Table 2*. In addition, the elastic modulus and Poisson's ratio of polypropylene are 1.85 GPa and 0.45, respectively. It should be noted that the CNTs are considered as a transversely isotropic material, while the polymer matrix is assumed to be isotropic. The average diameter of the CNTs is 50 nm. Furthermore, the interphase thickness and adhesion exponent in *Eq. (1)* are taken as 2.38 nm and 23.28, respectively.

Fig. 9 shows the comparison between the elastic modulus of the polypropylene-matrix nanocomposite obtained from the Mori–Tanaka method and experimental results. The present micromechanical model provides acceptable accuracy compared with the experimental data. *Fig. 9* also shows that increasing the CNT volume fraction in the polymer matrix increases the nanocomposite's elastic modulus.

Table 2. Mechanical properties of CNTs and epoxy resin.

Material	ELE_LEL (GPa)	ETE_TET (GPa)	vLv_LvL	vTv_TvT
CNT	800	49	0.16	0.45

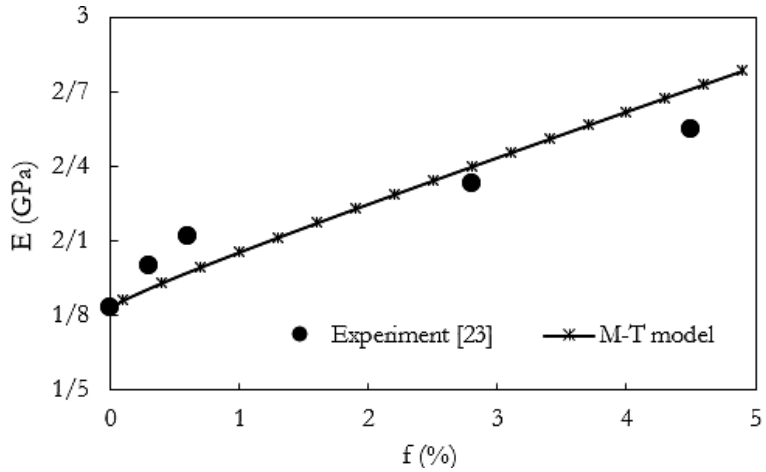

Fig. 9. Comparison between the Mori–Tanaka method and experimental results for the elastic modulus of a polypropylene-matrix nanocomposite reinforced with randomly distributed CNTs.

From the overall comparisons presented in *Figs. 7-9*, it can be confirmed that the proposed micromechanical model has acceptable accuracy. Therefore, it is suitable for extracting the mechanical properties of nanocomposites.

4.2 | Parametric Study of Mechanical Properties

In this section, the mechanical property relations of an epoxy shape-memory polymer nanocomposite reinforced with CNTs are derived. To account for temperature effects, the following relation gives the elastic modulus of the polymer matrix:

$$E_P = \frac{1}{\frac{\varphi_f}{E_i} + \frac{1-\varphi_f}{E_e}}, \tag{21}$$

where φ_f and E_e are are defined as follows:

$$E_e = kT, \qquad \varphi_f = 1 - \frac{1}{1 + c_f(T_h - T)^n}, \tag{22}$$

where T is the temperature. The remaining parameters in *Eqs. (21)* and *(22)* are given in *Table 3*. From *Eq. (21)*, it is clear that the elastic modulus of the polymer matrix is temperature-dependent; however, its Poisson's ratio is assumed to be constant and equal to 0.3, as shown in *Table 2*. In addition, the mechanical properties of single-walled CNTs of the (10,10) type are provided in *Table 4*.

Table 3. Properties of shape-memory polymer matrix for parametric study.

c_f (K^{-4})	T_h (K)	E_i (MPa)	k (MPa/K)	n	v
2.76×10^{-5}	358	813	2.64×10^{-2}	4	0.3

Table 4. Mechanical properties of (10,10) single-walled CNT.

E_L (GPa)	G_L (GPa)	v_L	E_T (GPa)	G_T (GPa)
1060	442	0.162	50	17

In *Figs. 10.(a)* and *10.(b)*, the variations of the longitudinal and transverse elastic moduli of the shape-memory polymer nanocomposite reinforced with aligned CNTs versus nanotube volume fraction are shown, respectively.

In these figures, the effects of considering and neglecting the interphase on the nanocomposite's elastic properties are also investigated. In other words, the results of the Mori–Tanaka micromechanical method are obtained both with and without considering the interphase between the nanotube and the polymer matrix. It is observed that increasing the volume fraction of CNTs in the polymer matrix leads to a linear increase in the elastic modulus of both aligned CNT-reinforced nanocomposites and randomly distributed CNT-reinforced nanocomposites.

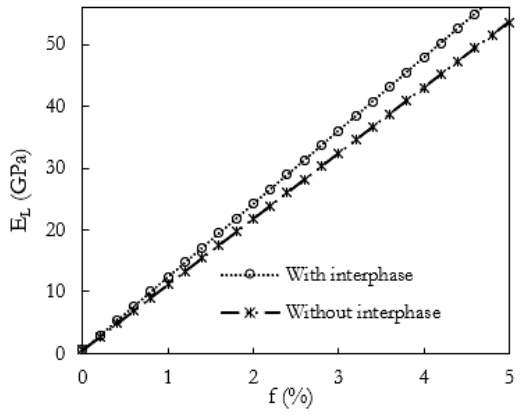

a.

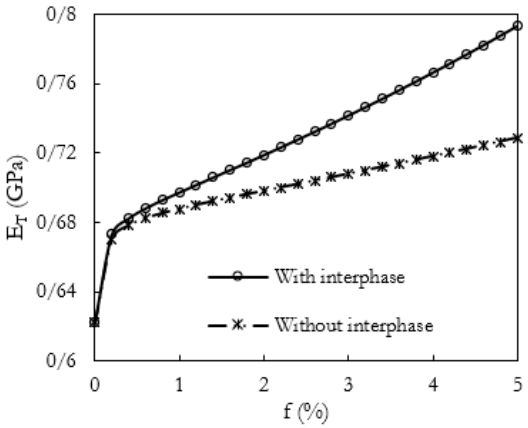

b.

Fig. 10. a. longitudinal, and b. transverse elastic modulus of a shape-memory polymer nanocomposite reinforced with aligned CNTs versus CNT volume fraction.

However, as shown in *Fig. 10.(b)*, the transverse elastic modulus of the aligned CNT-reinforced shape-memory polymer nanocomposite increases nonlinearly with increasing CNT volume fraction. On the other hand, as shown in *Fig. 10*, the nanocomposite's elastic modulus is higher when the interphase is included in the model than when it is neglected. This is because the mechanical properties of the interphase are higher than those of the polymer matrix. In fact, the properties of the interphase are functions of both the CNT and the polymer matrix properties. Therefore, it is expected that the mechanical properties of the interphase are lower than

those of the CNTs but higher than those of the polymer matrix. The results clearly show that the transverse elastic modulus of the aligned CNT-reinforced nanocomposite is most significantly affected by the interphase.

In *Figs. 11.(a)* and *11.(b)*, the variations of the longitudinal and transverse elastic moduli of the shape-memory polymer nanocomposite reinforced with aligned CNTs versus temperature are shown, respectively. In addition, *Fig. 11.(c)* presents the elastic modulus of the shape-memory polymer nanocomposite containing randomly distributed CNTs as a function of temperature. The temperature range is 260 K to 350 K. Furthermore, the effects of the interphase formed between the nanotube and the polymer matrix on the nanocomposite's elastic stiffness are investigated.

The modeling results indicate that the elastic modulus decreases with increasing temperature. According to *Fig. 11.(a)*, this reduction in the longitudinal elastic modulus of the aligned CNT-reinforced nanocomposite is very small, whereas, as shown in *Fig. 11.(b)*, the reduction in the transverse direction is significantly more pronounced. The decrease in elastic modulus with increasing temperature is due to the polymer matrix's elastic modulus decreasing with temperature, as shown in *Eq. (21)*.

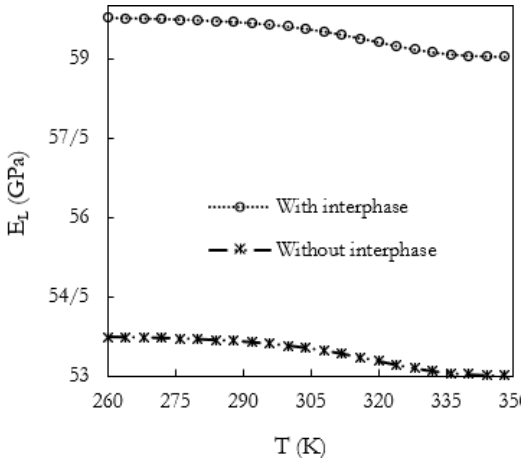

a.

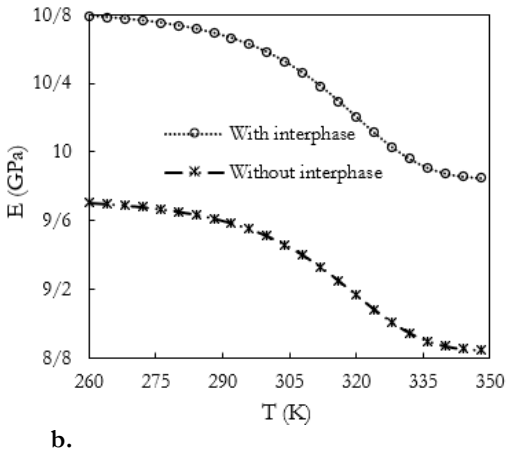

b.

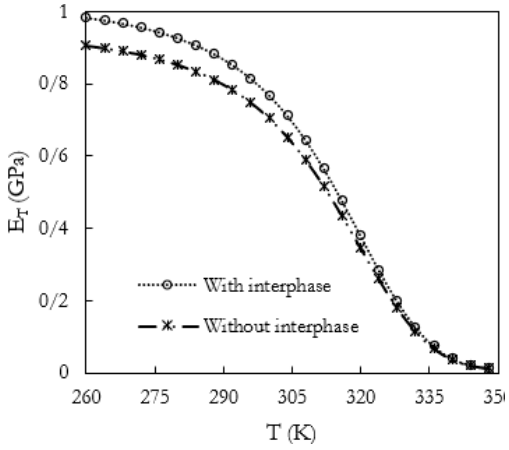

c.

Fig. 11. a. longitudinal and b. transverse elastic modulus of a shape-memory polymer nanocomposite reinforced with aligned CNTs versus temperature, and c. elastic modulus of a shape-memory polymer nanocomposite containing randomly distributed CNTs versus temperature.

From *Fig. 11*, it is observed that the mechanical properties of the nanocomposite are higher when the interphase is considered than when it is neglected.

Next, using the Mori–Tanaka micromechanical model, a parametric study is performed to investigate the effect of CNT diameter on the Young's modulus of the shape-memory polymer nanocomposite. In *Figs. 12.(a)* and *12.(b)*, the variations of the longitudinal and transverse elastic moduli of the shape-memory polymer nanocomposite reinforced with aligned CNTs versus CNT diameter are shown, respectively. In addition, *Fig. 12.(c)* presents the elastic modulus of the shape-memory polymer nanocomposite containing randomly distributed CNTs as a function of nanotube diameter.

The nanotube diameter is varied between 0.5 and 4 nm. Furthermore, in *Fig. 12*, two important parameters, namely temperature and interphase, are considered in evaluating the stiffness of the nanocomposite. The results are obtained at 298 K and 348 K.

From the results presented in *Fig. 12*, it is clear that, in the presence of the interphase, reducing the diameter of the CNTs significantly improves the mechanical properties of the nanocomposite. This is because decreasing the nanotube diameter increases the surface-to-volume ratio of the nanotubes and, consequently, the volume fraction of the interphase, which has higher mechanical properties than the polymer matrix. As a result, the overall properties of the nanocomposite are enhanced. As shown in *Fig. 12*, without considering the interphase, changes in nanotube diameter do not affect the nanocomposite's effective stiffness.

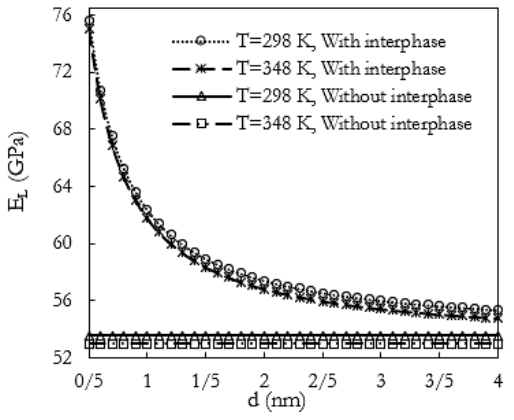

a.

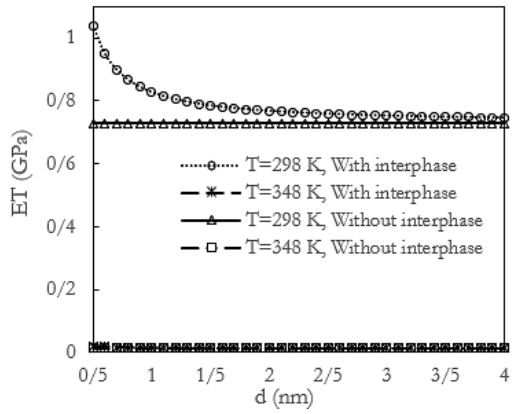

b.

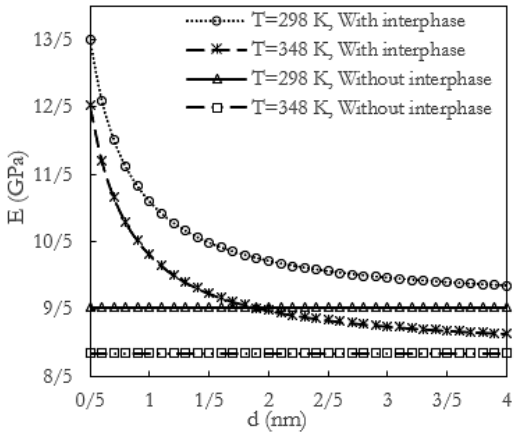

c.

Fig. 12. A. longitudinal and b transverse elastic modulus of a shape-memory polymer nanocomposite reinforced with aligned CNTs versus CNT diameter, and c. elastic modulus of a shape-memory polymer nanocomposite containing randomly distributed CNTs versus CNT diameter.

As shown above, the interphase significantly affects the nanocomposite's mechanical properties. Therefore, it is necessary to investigate the influence of its parameters on the nanocomposite's elastic stiffness.

In *Figs. 13.(a)* and *13.(b)*, the variations of the longitudinal and transverse elastic moduli of the shape-memory polymer nanocomposite reinforced with aligned CNTs versus interphase thickness (ti) are shown, respectively. In addition, *Fig. 13.(c)* presents the elastic modulus of the shape-memory polymer nanocomposite containing randomly distributed CNTs as a function of interphase thickness.

The interphase thickness ranges from 0.1 to 1.3 nm. Furthermore, the numerical results are obtained at four temperatures: 273 K, 298 K, 323 K, and 348 K.

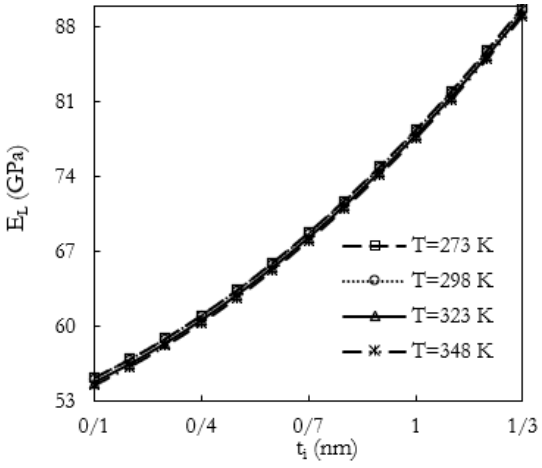

a.

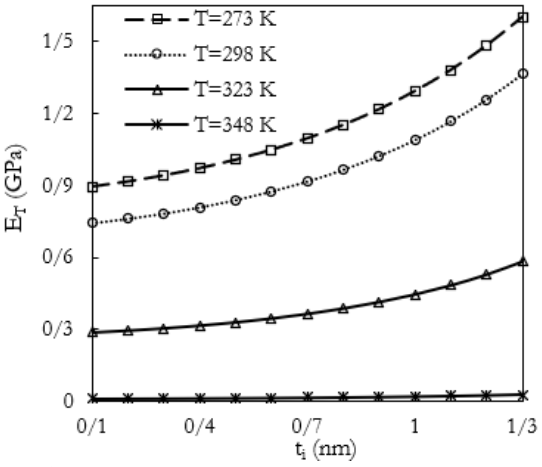

b.

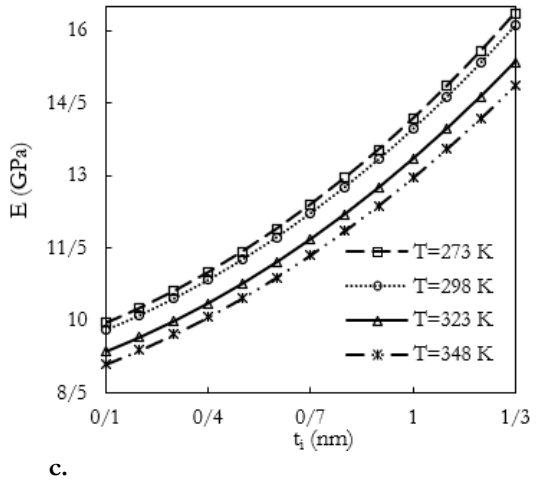

c.

Fig. 13. a. Longitudinal and b. transverse elastic modulus of a shape-memory polymer nanocomposite reinforced with aligned CNTs versus interphase thickness, and c. elastic modulus of a shape-memory polymer nanocomposite containing randomly distributed CNTs versus interphase thickness.

Fig. 13 shows that increasing the interphase thickness improves the nanocomposite's elastic properties. This is because increasing the interphase thickness increases the volume fraction of this region within the nanocomposite, thereby increasing its influence on the overall properties.

Another parametric study is devoted to investigating the effect of the interphase adhesion exponent (η) on the elastic properties of the nanocomposite. In *Figs. 14.(a)* and *14.(b)*, the variations of the longitudinal and transverse elastic moduli of the shape-memory polymer nanocomposite reinforced with aligned CNTs versus the interphase exponent are shown, respectively. In addition, *Fig. 14.(c)* presents the elastic modulus of the shape-memory polymer nanocomposite containing randomly distributed CNTs as a function of the interphase exponent.

The interphase adhesion exponent is varied between 0.01 and 95. The numerical results are obtained at four temperatures: 273 K, 298 K, 323 K, and 348 K.

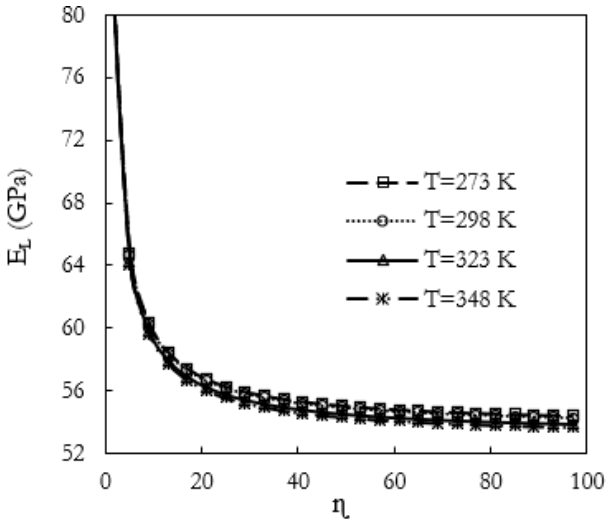

a.

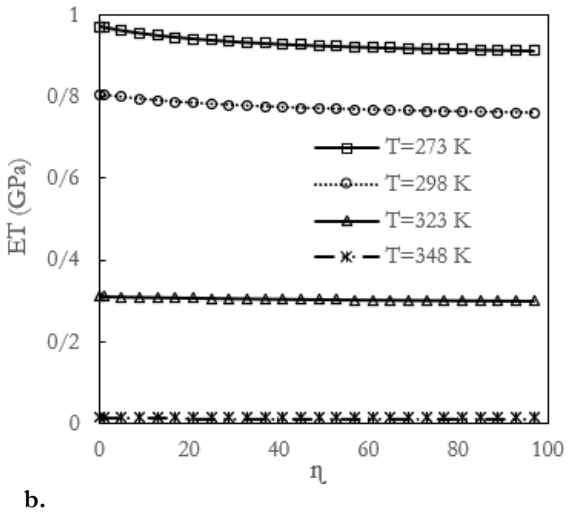

b.

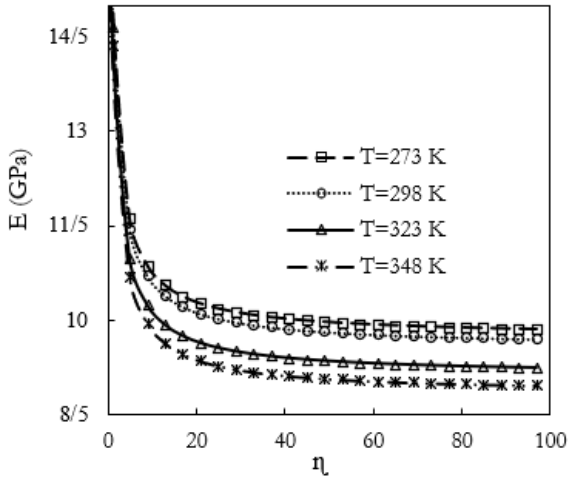

c.

Fig. 14. a. longitudinal and b. transverse elastic modulus of a shape-memory polymer nanocomposite reinforced with aligned CNTs versus interphase adhesion exponent, and c. elastic modulus of a shape-memory polymer nanocomposite containing randomly distributed CNTs versus interphase adhesion exponent.

As shown in *Fig. 14*, micromechanical modeling results indicate that variations in the interphase exponent can significantly alter the nanocomposite's final properties. These changes may be attributed to the functionalization of CNTs with different groups, such as alcohol-based functional groups. A decrease in the interphase exponent leads to an increase in the elastic stiffness of the nanocomposite. This is because, according to *Eq. (1)*, reducing the interphase exponent causes the mechanical properties of the interphase to become closer to those of the CNTs, which are significantly higher than those of the polymer matrix. This, in turn, results in an increase in the overall properties of the nanocomposite.

4.3 | Buckling Behavior Results of the Nanocomposite Beam

In this section, using the data obtained from the micromechanical analysis in Section 2, the buckling behavior of a beam made of an epoxy shape-memory polymer nanocomposite reinforced with CNTs is investigated using the FEM. The effects of volume fraction, nanotube distribution type, temperature, and interphase characteristics, including material properties and thickness, on the buckling response of the nanocomposite beam are studied. The beam length is 1 m, and its cross-sectional dimensions are 0.1 × 0.1 m.

In this section, the buckling behavior of the nanocomposite beam whose properties were derived in Section 2 is presented. *Table 5* shows the buckling loads of the nanocomposite beam for the first five modes at CNT volume fractions of 0, 1, 2, 3, 4, and 5% with the presence of the interphase. Similarly, *Table 6* presents the buckling loads of the nanocomposite beam for the first five modes at the same volume fractions but without considering the interphase.

The results of *Tables 5* and *6* clearly show that increasing the CNT volume fraction increases the buckling load of the beam made from the nanocomposite material. This is due to the nanocomposite's increased stiffness with increasing CNT content. It should be noted that the elastic modulus of CNTs is significantly higher than that of the polymer resin. For example, *Table 5* shows that the first-mode buckling load for the pure polymer beam (without CNTs) is 2,647,180 Pa. In contrast, for the nanocomposite beam containing 5% CNTs, it increases to 45,115,200 Pa.

Table 5. Buckling load (Pa) of the nanocomposite beam for different nanotube volume fractions with interphase (nanotube/resin system).

Volume Fraction (%)	0	1	2	3	4	5
Mode 1	2,647,180	11,212,300	19,693,700	28,167,400	36,640,700	45,115,200
Mode 2	2,647,180	11,212,300	19,693,700	28,167,400	36,640,700	45,115,200
Mode 3	4,390,150	18,594,800	32,660,500	46,713,500	60,765,800	74,820,300
Mode 4	4,390,150	18,594,800	32,660,500	46,713,500	60,765,800	74,820,300
Mode 5	13,856,900	58,691,900	103,088,000	147,445,000	191,799,000	236,159,000

Table 6. Buckling load (Pa) of the nanocomposite beam for different nanotube volume fractions without interphase (nanotube/resin system).

Volume Fraction (%)	0	1	2	3	4	5
Mode 1	2,647,180	10,285,800	17,860,300	25,426,600	32,989,600	40,550,800
Mode 2	2,647,180	10,285,800	17,860,300	25,426,600	32,989,600	40,550,800
Mode 3	4,390,150	17,058,300	29,620,000	42,168,200	54,710,800	67,250,500
Mode 4	4,390,150	17,058,300	29,620,000	42,168,200	54,710,800	67,250,500
Mode 5	13,856,900	53,842,100	93,491,100	133,098,000	172,687,000	212,267,000

Therefore, as an important result, adding CNTs to the beam can significantly delay buckling-induced failure. As expected from the three-dimensional modeling of the nanocomposite beam, the buckling loads in the first and second modes are identical. Similarly, the third and fourth modes also coincide.

Comparing the results of *Tables 5* and *6* shows that the presence of the interphase increases the buckling load. This is due to the interphase's higher stiffness relative to the polymer resin, which increases the overall stiffness of the structure.

The effect of temperature on the beam's buckling behavior is also significant. In *Tables 7* and *8*, the buckling loads of the nanocomposite beam for the first five modes at different temperatures (260, 280, 300, 320, and 340 K) are presented, with and without the interphase, respectively. These results are obtained for a CNT volume fraction of 3%.

The results of *Tables 7* and *8* clearly show that temperature variations have a significant effect on the mechanical behavior of the nanocomposite beam. Increasing temperature reduces the buckling load of the nanocomposite beam, as it decreases the material's stiffness. For example, *Table 7* shows that the first-mode buckling load at 260 K is 45,908,100 Pa, while at 340 K it decreases to 42,013,300 Pa.

Finally, the effect of CNT diameter on the buckling behavior of the nanocomposite beam is investigated. In *Table 9*, the buckling loads for the first five modes at different nanotube diameters (0.5, 1.5, 2.5, and 3.5 nm) with interphase at 298 K are presented. In *Table 10*, the corresponding results without interphase at 298 K are shown.

Table 7. Buckling load (Pa) of the nanocomposite beam for different temperatures with interphase (nanotube/resin system).

Temperature (K)	260	280	300	320	340
Mode 1	45,908,100	45,673,300	45,014,000	43,407,300	42,013,300
Mode 2	45,908,100	45,673,300	45,014,000	43,407,300	42,013,300
Mode 3	76,135,300	75,745,800	74,652,400	71,987,800	69,676,000
Mode 4	76,135,300	75,745,800	74,652,400	71,987,800	69,676,000
Mode 5	240,310,000	239,081,000	235,629,000	227,219,000	219,922,000
Temperature (K)	**260**	**280**	**300**	**320**	**340**
Mode 1	45,908,100	45,673,300	45,014,000	43,407,300	42,013,300
Mode 2	45,908,100	45,673,300	45,014,000	43,407,300	42,013,300
Mode 3	76,135,300	75,745,800	74,652,400	71,987,800	69,676,000
Mode 4	76,135,300	75,745,800	74,652,400	71,987,800	69,676,000
Mode 5	240,310,000	239,081,000	235,629,000	227,219,000	219,922,000

Table 8. Buckling load (Pa) of the nanocomposite beam for different temperatures without interphase (nanotube/resin system).

Temperature (K)	260	280	300	320	340
Mode 1	41,277,800	41,062,500	40,458,100	38,991,300	37,727,100
Mode 2	41,277,800	41,062,500	40,458,100	38,991,300	37,727,100
Mode 3	68,456,200	68,099,200	67,096,700	64,664,300	62,567,600
Mode 4	68,456,200	68,099,200	67,096,700	64,664,300	62,567,600
Mode 5	216,072,000	214,945,000	211,781,000	204,104,000	197,486,000

Table 9. Buckling load (Pa) of the nanocomposite beam for different nanotube diameters with interphase (nanotube/resin system).

Diameter (nm)	0.5	1.5	2.5	3.5
Mode 1	57,399,900	44,610,700	42,805,400	42,106,000
Mode 2	57,399,900	44,610,700	42,805,400	42,106,000
Mode 3	95,193,600	73,983,600	70,989,500	69,829,700
Mode 4	95,193,600	73,983,600	70,989,500	69,829,700
Mode 5	300,465,000	233,518,000	224,068,000	220,408,000
Diameter (nm)	**0.5**	**1.5**	**2.5**	**3.5**
Mode 1	57,399,900	44,610,700	42,805,400	42,106,000
Mode 2	57,399,900	44,610,700	42,805,400	42,106,000
Mode 3	95,193,600	73,983,600	70,989,500	69,829,700
Mode 4	95,193,600	73,983,600	70,989,500	69,829,700
Mode 5	300,465,000	233,518,000	224,068,000	220,408,000

Table 10. Buckling load (Pa) of the nanocomposite beam for different nanotube diameters without interphase (nanotube/resin system).

Diameter (nm)	0.5	1.5	2.5	3.5
Mode 1	40,550,800	40,550,800	40,550,800	40,550,800
Mode 2	40,550,800	40,550,800	40,550,800	40,550,800
Mode 3	67,250,500	67,250,500	67,250,500	67,250,500
Mode 4	67,250,500	67,250,500	67,250,500	67,250,500
Mode 5	212,267,000	212,267,000	212,267,000	212,267,000

The results in *Table 10* show that, in the presence of the interphase, changes in the CNT diameter have a noticeable effect on the buckling behavior of the nanocomposite. A reduction in nanotube diameter increases the buckling load of the nanocomposite beam. For instance, the first-mode buckling load is 57,399,900 Pa for a nanotube diameter of 0.5 nm, decreasing to 42,106,000 Pa for a diameter of 3.5 nm.

On the other hand, the results in *Table 10* clearly show that in the absence of the interphase, variations in nanotube diameter do not affect the buckling response of the nanocomposite structure.

Next, the effect of interphase thickness on the buckling behavior of the nanocomposite beam is investigated. In *Table 11*, the buckling loads of the nanocomposite beam for the first five modes at different interphase thicknesses (0.1, 0.4, 0.8, and 1.2 nm) at 298 K are presented. *Table 12* presents the corresponding results at 348 K. It is observed that variations in interphase thickness significantly affect the buckling response of the

nanocomposite beam. Finite element simulations indicate that increasing the interphase thickness leads to an increase in the buckling load of the structure. This is because the overall stiffness of the structure increases with increasing interphase thickness. For example, the first-mode buckling load is 41,702,300 Pa at an interphase thickness of 0.1 nm, increasing to 65,284,000 Pa at 1.2 nm.

Table 11. Buckling load (Pa) of the nanocomposite beam for different interphase thicknesses at 298 K.

Interphase Thickness (Nm)	0.1	0.4	0.8	1.2
Mode 1	41702300	46112700	54287400	65284000
Mode 2	41702300	46112700	54287400	65284000
Mode 3	69160300	76474600	90031600	108269000
Mode 4	69160300	76474600	90031600	108269000
Mode 5	218294000	241381000	284172000	341735000

Table 12. Buckling load (Pa) of the nanocomposite beam for different interphase thicknesses at 348 K.

Interphase thickness (nm)	0.1	0.4	0.8	1.2
Mode 1	38708000	42835600	50412500	60363600
Mode 2	38708000	42835600	50412500	60363600
Mode 3	64194400	71039600	83605500	100109000
Mode 4	64194400	71039600	83605500	100109000
Mode 5	202621000	224226000	263889000	315978000

In this section, the effect of the nanocomposite beam's geometric dimensions on its buckling response is investigated. *Table 13* presents the buckling loads for the first five modes for beam lengths of 0.5, 1, and 1.5 m. As expected, increasing the beam length reduces the buckling load. For example, the first-mode buckling load is 103106000 Pa for a beam length of 0.5 m, decreasing to 12961900 Pa for a length of 1.5 m.

Table 14 presents the buckling loads for different beam cross-sectional dimensions. The numerical results clearly indicate that increasing the cross-sectional area significantly increases the buckling load. For instance, the first-mode buckling load is 18555900 Pa for a beam with a cross-section of 0.08 × 0.08 m, while it increases to 39434200 Pa for a cross-section of 0.12 × 0.12 m.

One of the most important factors affecting convergence and the accuracy of the buckling results is the proper selection of element size and, consequently, the number of elements used in the finite element model. This issue is so critical that even with correct modeling procedures, inaccurate results may be obtained if mesh density is not properly selected. Therefore, a mesh convergence study is essential for the nanocomposite beam analysis.

Table 13. Buckling load (Pa) of the nanocomposite beam for different beam lengths.

Length (m)	0.5	1	1.5
Mode 1	103106000	28167400	12961900
Mode 2	103106000	28167400	12961900
Mode 3	161919000	46713500	21841300
Mode 4	161919000	46713500	21841300
Mode 5	489622000	147445000	69202600

Table 14. Buckling load (Pa) of the nanocomposite beam for different cross-sectional dimensions.

Cross-section (m²)	0.08 × 0.08	0.10 × 0.10	0.12 × 0.12
Mode 1	18555900	28167400	39434200
Mode 2	18555900	28167400	39434200
Mode 3	31140100	46713500	64544500
Mode 4	31140100	46713500	64544500
Mode 5	98213900	147445000	203934000

Table 15 presents the buckling loads of the nanocomposite beam for the first five modes corresponding to different numbers of finite elements used in the simulation. As observed, when the number of elements exceeds 5000, the results show good agreement and convergence, indicating mesh-independent and reliable solutions.

Table 15. Buckling load (Pa) of the nanocomposite beam for different numbers of finite elements.

Number Of Elements	5312	46541	95060
Mode 1	28427700	28167400	27871300
Mode 2	28427700	28167400	27871300
Mode 3	47258900	46713500	46089100
Mode 4	47258900	46713500	46089100
Mode 5	148482000	147445000	146287000

Table 16 presents a comparison of the buckling loads for the first five modes of a nanocomposite beam with a solid square cross-section and a hollow square cross-section with a wall thickness of 0.01 m. The results are obtained for a CNT volume fraction of 3%.

As shown in *Table 16*, the buckling load of the solid square cross-section beam is higher than that of the hollow beam up to the fourth mode. However, in the fifth mode, the hollow square beam exhibits a higher buckling load compared to the solid beam.

For the fifth mode, the buckling load is 147,445,000 Pa for the solid beam, while it increases to 166,743,000 Pa for the hollow beam.

Table 16. Comparison of buckling load for solid and hollow square cross-section nanocomposite beams.

Mode	Solid Section	Hollow Section
Mode 1	28167400	20832400
Mode 2	28167400	20832400
Mode 3	46713500	27589100
Mode 4	46713500	27589100
Mode 5	147445000	166743000

Table 17 presents the buckling loads for the first five modes of a nanocomposite beam with a solid circular cross-section (diameter = 0.1 m, length = 1 m) and a hollow circular beam with an outer diameter of 0.1 m, wall thickness of 0.01 m, and length of 1 m.

Table 17. Buckling load (Pa) comparison for solid and hollow circular nanocomposite beams Mode.

Mode	Solid Section	Hollow Section
Mode 1	21829400	19309300
Mode 2	21829400	19309300
Mode 3	36574100	26500200
Mode 4	36574100	26500200
Mode 5	115339000	136560000

5 | Conclusion

Reinforcement of polymer matrix nanocomposites with CNTs is a modern approach to enhancing their mechanical properties for advanced engineering applications, particularly in the aerospace industry. Owing to the exceptional properties of CNTs, such as extremely high stiffness and strength, low thermal expansion coefficient, and low density, these nanocomposites exhibit significantly improved mechanical performance compared to conventional composites.

To analyze the mechanical behavior of structures made of CNT-reinforced nanocomposites, it is first necessary to determine their effective material properties. Therefore, in this study, the analytical Mori–Tanaka micromechanical model was first employed to extract the effective mechanical properties of CNT-reinforced nanocomposites. CNTs were initially modeled as aligned reinforcements, and isotropic equivalent properties such as Young's modulus and Poisson's ratio were obtained using homogenization relations. A continuous equivalent solid medium, referred to as the interphase, was introduced to model van der Waals interactions between nanotube atoms and the polymer matrix within the micromechanical modeling framework. Subsequently, the buckling behavior of nanocomposite beams was investigated using the FEM. For beam meshing, a 20-node quadratic brick element (C3D20) was used.

Several comparisons were performed between the micromechanical model predictions and experimental data, demonstrating that the proposed model accurately predicts experimental results. The effects of various parameters, including CNT volume fraction, nanotube diameter, temperature, interphase thickness, and interphase adhesion exponent, on the longitudinal and transverse elastic moduli, as well as the isotropic equivalent elastic modulus, were investigated. In general, increasing the CNT volume fraction leads to an increase in the Young's modulus of the nanocomposite. It was also found that the transverse elastic modulus of the shape-memory polymer nanocomposite reinforced with aligned CNTs increases nonlinearly with increasing nanotube volume fraction. Furthermore, reducing the nanotube diameter improves mechanical properties by increasing the contribution of the interphase region. In the absence of the interphase, variations in nanotube length have no significant effect on the effective stiffness of the nanocomposite. Increasing the interphase thickness also enhances the nanocomposite's elastic properties, as a larger interphase volume fraction contributes more significantly to the overall material response.

The structural analysis results indicated that increasing the CNT volume fraction increases the buckling load of the nanocomposite beam. Therefore, as a key finding, the addition of CNTs can significantly delay buckling failure in beams. The results also showed that increasing temperature reduces the buckling load because the nanocomposite's stiffness decreases. Moreover, finite element analysis revealed that for a solid square cross-section beam, the buckling load is higher than that of a hollow square beam up to the fourth mode. However, in the fifth mode, the hollow square beam exhibits a higher buckling load compared to the solid beam.

Funding

This work was carried out without financial support from any public, commercial, or non-profit organizations.

Data Availability

The data are available from the corresponding author upon reasonable request.

Conflict of Interest

There are no competing interests to declare.

Consent for Publication

The authors confirm consent for the publication of this work.

References

[1] Eken, A. E., Tozzi, E. J., Klingenberg, D. J., & Bauhofer, W. (2012). Combined effects of nanotube aspect ratio and shear rate on the carbon nanotube/polymer composites. *Polymer*, *53*(20), 4493–4500. https://doi.org/10.1016/j.polymer.2012.07.045

[2] Schadler, L. S., Giannaris, S. C., & Ajayan, P. M. (1998). Load transfer in carbon nanotube epoxy composites. *Applied physics letters*, *73*(26), 3842–3844. https://doi.org/10.1063/1.122911

[3] Shokrieh, M. M., Daneshvar, A., & Akbari, S. (2014). Reduction of thermal residual stresses of laminated polymer composites by addition of carbon nanotubes. *Materials & design*, *53*, 209–216. https://doi.org/10.1016/j.matdes.2013.07.007

[4] Kaleemullah, M., Khan, S. U., & Kim, J. K. (2012). Effect of surfactant treatment on thermal stability and mechanical properties of CNT/polybenzoxazine nanocomposites. *Composites science and technology*, *72*(16), 1968–1976. https://doi.org/10.1016/j.compscitech.2012.08.020

[5] Stern, T., & Marom, G. (2024). Fracture mechanisms and toughness in polymer nanocomposites: A brief review. *Journal of composites science*, *8*(10), 1–16. https://doi.org/10.3390/jcs8100395

[6] Gupta, A. K., & Harsha, S. P. (2016). Analysis of mechanical properties of carbon nanotube reinforced polymer composites using multi-scale finite element modeling approach. *Composites part b: Engineering*, *95*, 172–178. https://doi.org/10.1016/j.compositesb.2016.04.005

[7] Malik, H., He, J., Zhang, H., Liu, Y., & Yu, J. (2025). Computational insights into PAN-based carbon fiber advancements: Simulation techniques, microstructural-property relationship, and future directions. *International materials reviews*, *70*(5), 422–462. https://doi.org/10.1177/09506608251337725

[8] Mortazavi, B., Bardon, J., & Ahzi, S. (2013). Interphase effect on the elastic and thermal conductivity response of polymer nanocomposite materials: 3D finite element study. *Computational materials science*, *69*, 100–106. https://doi.org/10.1016/j.commatsci.2012.11.035

[9] Joshi, P., & Upadhyay, S. H. (2014). Effect of interphase on elastic behavior of multiwalled carbon nanotube reinforced composite. *Computational materials science*, *87*, 267–273. https://doi.org/10.1016/j.commatsci.2014.02.029

[10] Sahu, R., Harursampath, D., & Ponnusami, S. A. (2024). Mechanical behaviour of carbon nanotube composites: A review of various modelling techniques. *Journal of composite materials*, *58*(6), 791–825. https://doi.org/10.1177/00219983231213967

[11] Wan, H., Delale, F., & Shen, L. (2005). Effect of CNT length and CNT-matrix interphase in carbon nanotube (CNT) reinforced composites. *Mechanics research communications*, *32*(5), 481–489. https://doi.org/10.1016/j.mechrescom.2004.10.011

[12] Karimi, M., Ghajar, R., & Montazeri, A. (2017). Investigation of nanotubes' length and their agglomeration effects on the elastoplastic behavior of polymer-based nanocomposites. *Journal of science and technology of composites*, *4*(2), 229-240. (**In Persian**). https://jstc.iust.ac.ir/article_27104_en.html

[13] Tamayo-Vegas, S., Muhsan, A., Liu, C., Tarfaoui, M., & Lafdi, K. (2022). The effect of agglomeration on the electrical and mechanical properties of polymer matrix nanocomposites reinforced with carbon nanotubes. *Polymers*, *14*(9), 1–17. https://doi.org/10.3390/polym14091842

[14] Hammerand, D. C., Seidel, G. D., & Lagoudas, D. C. (2007). Computational micromechanics of clustering and interphase effects in carbon nanotube composites. *Mechanics of advanced materials and structures*, *14*(4), 277–294. https://doi.org/10.1080/15376490600817370

[15] Zhang, J., & He, C. (2008). A three-phase cylindrical shear-lag model for carbon nanotube composites. *Acta mechanica*, *196*(1), 33–54. https://doi.org/10.1007/s00707-007-0489-x

[16] Mehrdad Shokrieh, M., Mosalmani, R., & Soveity, S. (2014). An investigation on effects of aspect ratio of representative volume element on elastic modulus of a carbon nanotubes reinforced polymer. *Modares mechanical engineering*, *14*(9), 107-116. (**In Persian**). https://mme.modares.ac.ir/article_8127.html?lang=en

[17] Mahmoodi, M., & Vakilifard, M. (2016). Electro-thermo-mechanical behavior modeling of short CNT reinforced piezo-polymeric composite. *Modares mechanical engineering*, *16*(4), 67-76. (**In Persian**). https://mme.modares.ac.ir/article_9189.html?lang=en

[18] Tsai, J. L., Tzeng, S. H., & Chiu, Y. T. (2010). Characterizing elastic properties of carbon nanotubes/polyimide nanocomposites using multi-scale simulation. *Composites part b: engineering*, *41*(1), 106–115. https://doi.org/10.1016/j.compositesb.2009.06.003

[19] Tserpes, K. I., & Papanikos, P. (2005). Finite element modeling of single-walled carbon nanotubes. *Composites part b: engineering*, *36*(5), 468–477. https://doi.org/10.1016/j.compositesb.2004.10.003

[20] Rossi, M., & Meo, M. (2009). On the estimation of mechanical properties of single-walled carbon nanotubes by using a molecular-mechanics based FE approach. *Composites science and technology*, *69*(9), 1394–1398. https://doi.org/10.1016/j.compscitech.2008.09.010

[21] Ansari, R., Ajori, S., & Ameri, A. (2014). Elastic and structural properties and buckling behavior of single-walled carbon nanotubes under chemical adsorption of atomic oxygen and hydroxyl. *Chemical physics letters*, *616–617*, 120–125. https://doi.org/10.1016/j.cplett.2014.10.036

[22] Thostenson, E. T., & Chou, T. W. (2003). On the elastic properties of carbon nanotube-based composites: modelling and characterization. *Journal of physics d: Applied physics*, *36*(5), 573. https://doi.org/10.1088/0022-3727/36/5/323

[23] Han, Y., & Elliott, J. (2007). Molecular dynamics simulations of the elastic properties of polymer/carbon nanotube composites. *Computational materials science*, *39*(2), 315–323. https://doi.org/10.1016/j.commatsci.2006.06.011

[24] Griebel, M., & Hamaekers, J. (2004). Molecular dynamics simulations of the elastic moduli of polymer–carbon nanotube composites. *Computer methods in applied mechanics and engineering*, *193*(17), 1773–1788. https://doi.org/10.1016/j.cma.2003.12.025

[25] Wang, J. F., & Liew, K. M. (2015). On the study of elastic properties of CNT-reinforced composites based on element-free MLS method with nanoscale cylindrical representative volume element. *Composite structures*, *124*, 1–9. https://doi.org/10.1016/j.compstruct.2015.01.006

[26] Pan, J., Bian, L., Zhao, H., & Zhao, Y. (2016). A new micromechanics model and effective elastic modulus of nanotube reinforced composites. *Computational materials science*, *113*, 21–26. https://doi.org/10.1016/j.commatsci.2015.11.009

[27] Imani Yengejeh, S., Kazemi, S. A., & Öchsner, A. (2017). Carbon nanotubes as reinforcement in composites: A review of the analytical, numerical and experimental approaches. *Computational materials science*, *136*, 85–101. https://doi.org/10.1016/j.commatsci.2017.04.023

[28] Karimi, M., Ghajar, R., & Montazeri, A. (2018). A novel interface-treated micromechanics approach for accurate and efficient modeling of CNT/polymer composites. *Composite structures*, *201*, 528–539. https://doi.org/10.1016/j.compstruct.2018.05.140

[29] Vodenitcharova, T., & Zhang, L. C. (2006). Bending and local buckling of a nanocomposite beam reinforced by a single-walled carbon nanotube. *International journal of solids and structures*, *43*(10), 3006–3024. https://doi.org/10.1016/j.ijsolstr.2005.05.014

[30] Shen, H.-S. (2011). Postbuckling of nanotube-reinforced composite cylindrical shells in thermal environments, Part II: Pressure-loaded shells. *Composite structures*, *93*(10), 2496–2503. https://doi.org/10.1016/j.compstruct.2011.04.005

[31] Torabi, J., Bazdid-Vahdati, M., & Ansari, R. (2015). Thermal buckling of functionally graded carbon nanotube-reinforced composite conical shells. *Modares mechanical engineering*, *15*(10), 137-146. (**In Persian**). https://mme.modares.ac.ir/article_8893.html?lang=en

[32] Zhu, P., Lei, Z. X., & Liew, K. M. (2012). Static and free vibration analyses of carbon nanotube-reinforced composite plates using finite element method with first order shear deformation plate theory. *Composite structures*, *94*(4), 1450–1460. https://doi.org/10.1016/j.compstruct.2011.11.010

[33] Lei, Z. X., Liew, K. M., & Yu, J. L. (2013). Buckling analysis of functionally graded carbon nanotube-reinforced composite plates using the element-free kp-Ritz method. *Composite structures*, *98*, 160–168. https://doi.org/10.1016/j.compstruct.2012.11.006

[34] Jafari Mehrabadi, S., Sobhani Aragh, B., Khoshkhahesh, V., & Taherpour, A. (2012). Mechanical buckling of nanocomposite rectangular plate reinforced by aligned and straight single-walled carbon nanotubes. *Composites part b: Engineering*, *43*(4), 2031–2040. https://doi.org/10.1016/j.compositesb.2012.01.067

[35] Shaat, M., Mahmoud, F. F., Gao, X. L., & Faheem, A. F. (2014). Size-dependent bending analysis of Kirchhoff nano-plates based on a modified couple-stress theory including surface effects. *International journal of mechanical sciences*, *79*, 31–37. https://doi.org/10.1016/j.ijmecsci.2013.11.022

[36] Malekzadeh, P., & Shojaee, M. (2013). Buckling analysis of quadrilateral laminated plates with carbon nanotubes reinforced composite layers. *Thin-walled structures*, *71*, 108–118. https://doi.org/10.1016/j.tws.2013.05.008

[37] Mohammadimehr, M., Mohandes, M., & Moradi, M. (2016). Size dependent effect on the buckling and vibration analysis of double-bonded nanocomposite piezoelectric plate reinforced by boron nitride nanotube based on modified couple stress theory. *Journal of vibration and control*, *22*(7), 1790–1807. https://doi.org/10.1177/1077546314544513

[38] Ansari, R., Torabi, J., & Shojaei, M. F. (2017). Buckling and vibration analysis of embedded functionally graded carbon nanotube-reinforced composite annular sector plates under thermal loading. *Composites part b: engineering*, *109*, 197–213. https://doi.org/10.1016/j.compositesb.2016.10.050

[39] Farzam, A., & Hassani, B. (2018). Thermal and mechanical buckling analysis of FG carbon nanotube reinforced composite plates using modified couple stress theory and isogeometric approach. *Composite structures*, *206*, 774–790. https://doi.org/10.1016/j.compstruct.2018.08.030

[40] Shirasu, K., Tamaki, I., Yamamoto, G., & Hashida, T. (2019). Mechanical and thermal expansion properties of aligned carbon nanotube reinforced epoxy composites. *Mechanical engineering journal*, *6*(3), 12–19. https://doi.org/10.1299/mej.19-00012